JOURNAL OF SURGICAL RESEARCH 187 (2014) 458–465

Available online at www.sciencedirect.com

ScienceDirect

journal homepage: www.JournalofSurgicalResearch.com

Small animal magnetic resonance imaging: an efficient tool to assess liver volume and intrahepatic vascular anatomy

Emmanuel Melloul, MD,[a] *Dimitri A. Raptis, MD, PhD,*[a] *Andreas Boss, MD, PhD,*[b] *Thomas Pfammater, MD,*[b] *Christoph Tschuor, MD,*[a] *Yinghua Tian, MD,*[a] *Rolf Graf, PhD,*[a] *Pierre-Alain Clavien, MD, PhD,*[a] *and Mickael Lesurtel, MD, PhD*[a,*]

[a] *Department of Surgery, Laboratory of the Swiss Hepato-Pancreato-Biliary (HPB) and Transplantation Center, University Hospital Zurich, Zurich, Switzerland*

[b] *Department of Radiology, University Hospital Zurich, Zurich, Switzerland*

ARTICLE INFO

Article history:
Received 29 June 2013
Received in revised form
28 October 2013
Accepted 11 November 2013
Available online 16 November 2013

Keywords:
Magnetic resonance imaging
Liver hypertrophy
Liver regeneration
Portography
Portal vein embolization
Hepatectomy

ABSTRACT

Background: To develop a noninvasive technique to assess liver volumetry and intrahepatic portal vein anatomy in a mouse model of liver regeneration.

Materials and methods: Fifty-two C57BL/6 male mice underwent magnetic resonance imaging (MRI) of the liver using a 4.7 T small animal MRI system after no treatment, 70% partial hepatectomy (PH), or selective portal vein embolization. The protocol consisted of the following sequences: three-dimensional–encoded spoiled gradient-echo sequence (repetition time per echo time 15 per 2.7 ms, flip angle 20°) for volumetry, and two-dimensional –encoded time-of-flight angiography sequence (repetition time per echo time 18 per 6.4 ms, flip angle 80°) for vessel visualization. Liver volume and portal vein segmentation was performed using a dedicated postprocessing software. In animals with portal vein embolization, portography served as reference standard. True liver volume was measured after sacrificing the animals. Measurements were carried out by two independent observers with subsequent analysis by the Cohen κ-test for interobserver agreement.

Results: MRI liver volumetry highly correlated with the true liver volume measurement using a conventional method in both the untreated liver and the liver remnant after 70% PH with a high interobserver correlation coefficient of 0.94 (95% confidence interval, 0.80–0.98 for untreated liver [$P < 0.001$] and 0.90–0.97 after 70% PH [$P < 0.001$]). The diagnostic accuracy of magnetic resonance angiography for the occlusion of one branch of the portal vein was 0.95 (95% confidence interval, 0.84–1). The level of agreement between the two observers for the description of intrahepatic vascular anatomy was excellent (Cohen κ value = 0.925).

Conclusions: This protocol may be used for noninvasive liver volumetry and visualization of portal vein anatomy in mice. It will serve the dynamic study of new strategies to enhance liver regeneration *in vivo*.

* *Corresponding author*. Department of surgery, University Hospital Zurich, Raemistrasse 100, CH-8091 Zurich, Switzerland. Tel.: +41 44 2552300; fax: +41 44 2554449.

E-mail address: mickael.lesurtel@usz.ch (M. Lesurtel).

0022-4804/$ – see front matter © 2014 Elsevier Inc. All rights reserved.
http://dx.doi.org/10.1016/j.jss.2013.11.1079

1. Introduction

The assessment of liver volume and perfusion is paramount in many clinical situations. It is extensively used in the preoperative setting before major liver resection and living donor liver transplantation to measure the future remnant liver (FRL) and prevent liver insufficiency. Indeed, postoperative insufficient functional liver mass typically leads to death of the patients within a few days [1]. To overcome this issue, one protective strategy is to occlude a main branch of the portal vein before surgery to induce hypertrophy of the FRL [2–7]. This requires optimal monitoring of the changes in liver volume and a complete picture of the intrahepatic vascular anatomy.

A number of animal models have been developed to study liver regeneration, including partial hepatectomy (PH). Up to now, the intrahepatic vascular anatomy is studied by repetitive x-ray imaging of animals after intravenous contrast injection (i.e., portography), which is an invasive procedure [4], technically demanding, and hence seldom used. Because liver regeneration is a dynamic process, important parameters might be lost or altered, if analyzed after having sacrificed animals. Moreover, a large number of animals are usually required for such experiments. Another method is the contrast-enhanced microscopic computed tomography (microCT) [8,9]. However, this method is limited by the need of contrast injection to differentiate soft tissues and body fluids [8].

Magnetic resonance imaging (MRI) is claimed to be a good alternative compared with a conventional method (i.e., measurements of volume *ex vivo* after sacrificing animals) to assess organ and tumor volumes in animal models [10,11]. However, data on mouse liver are scarce and there is lack of standardization [12–14]. Currently, new advances in imaging techniques provide unique possibilities to visualize the internal structure of organs and to collect systematic imaging data. New open source software, such as OsiriX (Pixmeo, Geneva, Switzerland), was developed to analyze imaging resources and give an accurate visual representation of these data [15]. The use of such software associated with the small animal MRI may contribute to the development of new methods for morphologic analysis of organs in mice and improve the tools available to study potential proregenerative agents in the liver. In addition, using MRI, animals can act as their own controls in repetitive measurements. Finally, a significant reduction in the number of animals used for experimentation would be achieved, and a decrease in interference with animal well-being and physiology status related to surgery required for conventional methods.

This study aimed at exploring the efficacy of small animal MRI to assess liver hypertrophy during liver regeneration after PH and modifications of intrahepatic vascular anatomy after portal vein occlusion in mice.

2. Materials and methods

2.1. Animals

All experiments were performed in 8–12-wk-old C57BL/6 male mice (Harlan, Horst, The Netherlands). Animals were housed in the animal facility of the University Hospital of Zurich with unrestricted access to standard chow and water. All experiments were approved by the Veterinary Office of Zurich and were performed in accordance with the institutional animal care guidelines.

2.2. Surgical procedures and anesthesia

All surgical procedures were performed between 8 and 12 h. All interventions were performed under constant isoflurane inhalation for surgery and MRI. For portography, an intraperitoneal bolus injection of pentobarbital (5 mg/kg body weight) was used as anesthesia to facilitate the transfer of animals from the operating room to imaging facilities. As analgesic, buprenorphine (0.1 mg/kg body weight) was applied subcutaneously and repeated 8–12 h later if required. After surgery, all animals were allowed to recover on a heating pad.

Seventy percent PH consisted of removal of the middle and left liver lobes with standard microsurgical techniques as described previously with some adaptations [16]. Briefly, the abdomen was opened by a midline incision. The left and middle lobes were ligated with a silk thread and resected. The gallbladder was also removed after ligation of the cystic duct. Finally, the abdomen was closed with a silk running suture. Sham surgery consisted of opening the abdominal cavity and liver mobilization without lobe resection.

Portal vein embolization (PVE) and portography procedures started with an abdominal midline incision. The peritoneal cavity was opened and the liver was freed from its ligaments. For portography, a puncture of the central portal vein was performed with a 29-gauge insulin needle (BD, Allschwil, Basel, Switzerland) attached to a 1-mL syringe connected to a butterfly tube . Vascular opacification (Fig. 1A) was performed with Sodium and Meglumine Ioxitalamate contrast agent (1:4 diluted with 0.9% NaCl: 0.25 mL Sodium and Meglumine Ioxitalamate + 0.75 mL NaCl 0.9%). At the end of the portography, the needle was removed from the central portal vein and hemostasis was achieved by the pressure on the puncture point. Seventy percent PVE was performed after blocking the portal branches to the caudate and right lobes with vascular clamps (Aesculap; Ref FE710K, B Braun, Melsungen AG, Germany). A puncture of the central portal vein was then performed with a 29-gauge insulin needle (BD) attached to a 1-mL syringe filled with 10 μL of microspheres made from trisacryl cross linked with gelatin (Embosphere, Biosphere Medical SA, Rockland, MA). Portography was then performed to confirm the occlusion of portal vessels (Fig. 1B).

2.3. Magnetic resonance imaging

Anesthetized mice were fixed to a warming pad in the ventral position. MRI was performed with a 4.7 T small animal magnetic resonance imager (Pharmascan; Bruker Biospin, Ettlingen, Germany) using a linearly polarized birdcage whole-body mouse coil. The protocol consisted after gradient-echo localizers in all three directions of the following sequences: a three-dimensional (3D)–encoded spoiled gradient-echo sequence with repetition time 15 ms, echo time 2.7 ms, flip angle 20°, field-of-view 24 × 30 × 30 mm^3, matrix size 256 × 256 × 128, resolution 0.09 × 0.117 × 0.234 mm^3, 7

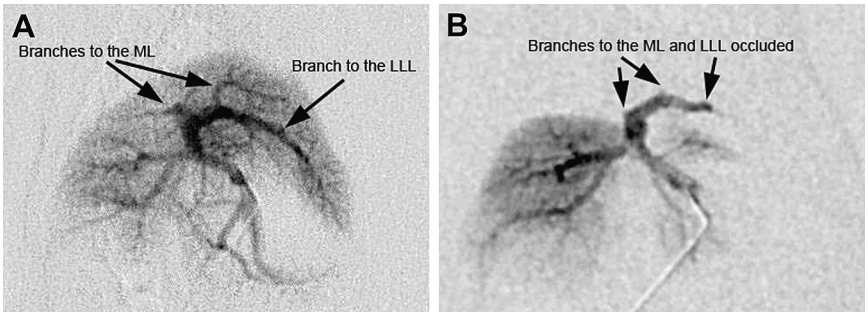

Fig. 1 – Portography before (A) and after (B) PVE in a single mouse. A small 29-gauge catheter was used to puncture the main trunk of the portal vein and to perform the portography. (B) The portal vein branches to the left lateral lobe (LLL) and the median lobe (ML) are occluded by Embospheres.

averages, total acquisition time 42 min for liver volumetry, and a 2D-encoded time-of-flight angiography sequence with repetition time 18 ms, echo time 6.4 ms, flip angle 80°, field-of-view 26 × 28 mm, matrix size 384 × 384, in-plane resolution 0.07 × 0.07 mm, slice thickness 0.63 mm, 7 averages, total acquisition time 30 min for portal vein visualization.

2.4. *MRI liver volume measurement*

Borders of the liver were manually drawn (region of interest, ROI) in every T1 sequence performed in each 0.23-mm-thick magnetic resonance slice by two independent blinded examiners (E.M., D.A.R.). The total liver volume was measured by a dedicated software from the MRI computing system (ParaVision, Bruker, Ettlingen, Germany). This software allows quantitative ROI analysis. According to the Cavalieri method [17], addition of all measured liver section surfaces (ROI) results in total liver volume (area [mm^2] × slice thickness) [18].

2.5. *OsiriX software*

OsiriX is an open source image processing software dedicated to the Digital Imaging and Communications in Medicine (DICOM) produced by imaging equipment (such as MRI and CT scan). This software has been specifically designed for navigation and visualization of multimodality and multidimensional images (free access at http://www.osirix-viewer.com/OsiriX3.9.1.pkg.zip). We converted the image data produced by the MRI into DICOM files with the use of the Bruker2 DICOM Converter (http://www.mricro.com). DICOM images were then analyzed using the OsiriX software and 3D reconstruction of the portal vein was performed.

2.6. *True liver volume measurements*

True liver volume was measured using a water displacement volumetry device as described [19]. Briefly, this system consists of the following three connected vessels: (A) vessel for the placement of liver, (B) vessel used for calibration, reading error 0.005 mL, and (C) vessel used for the true volume measurement, reading error 0.005 mL, filled with water. Vessel C is gauged and calibrated to determine differences in volume displacement. By placing the liver in vessel A, the liquid level in recipients B and C also rises. The water levels are then marked in vessels A and B. Vessel C is lowered until the water in vessel B has reached its original level. The water displacement in C corresponds with the volume of the liver.

2.7. *Histology and immunohistochemistry*

Liver tissue was fixed in a 4% buffered formaldehyde solution, embedded in paraffin, and then stained with hematoxylin-eosin and sirius red using standard histologic techniques. To assess hepatocyte proliferation during liver regeneration, sections were immunostained for Ki-67 (monoclonal rabbit clone SP; Abcam, The Hague, The Netherlands) and phosphorylated histone 3 (pH3) according to the manufacturer's instructions. All immunostainings were counterstained with hematoxylin. Ki-67 and pH3 positive cells were counted in at least five randomly selected high-power fields (×20) per slide.

2.8. *Assessment of diagnosis accuracy of magnetic resonance angiography*

Two independent examiners from our laboratory (C.T. and D.A.R.) assessed the imaging of 16 mice that underwent consecutively magnetic resonance angiography (MRA) and portography, with or without the previous occlusion of branches of the portal vein. First, they were asked to assess the occlusion status of the portal vein (occluded or not) and the intrahepatic vascular anatomy on the portography and the MRA. For both imaging techniques, up to five questions per image were asked in addition to the embolization status for the assessment of intrahepatic vascular anatomy (e.g., recognition of the main trunk or branches to the right lobe [RL], caudate lobe [CL], medial lobe [ML], left lateral lobe [LLL], and inferior or superior right lobes). The portography was used as gold standard. Before the assessment by the two observers, one experienced hepatic microsurgeon (E.M.) and one radiologist (T.P.) agreed on the description of intrahepatic portal vein branches after having analyzed the same images from portography and MRA in wild-type mice.

2.9. *Statistics*

Data are expressed as the mean ± standard deviation (SD). Linear regression analysis was performed from the data obtained to correlate MRI volumetry findings with the true liver

volume determined at autopsy. Statistical analysis was performed on SPSS Version 20 for Mac (SPSS 20; IBM Company, Chicago, IL). Categorical data were compared with the Fisher exact test or the χ^2 test and continuous variables with the Student *t-test* or one-way analysis of variance, whichever will be appropriate. Receiver operating characteristic curve analysis was used to assess the diagnosis accuracy of MRA for embolization of the portal vein tributaries. Measurement of the level of agreement between the two examiners (C.T. and D.A.R.) was performed with the Cohen κ-test for the different items used to assess the intrahepatic architecture of the portal vein (i.e., branches to the RL, CL, LLL, and ML). This measure calculates the degree of agreement in classification over that which would be expected by chance and is scored as a number between 0 and 1. A κ value of >0.8 indicates excellent, 0.6–0.8 good, 0.4–0.6 moderate, 0.2–0.4 poor, and <0.2 no agreement. All *P* values were two-sided and were considered statistically significant if $P \leq 0.05$.

3. Results

3.1. Small animal MRI and native liver volumetry

MRI liver volumetry highly correlated with the true liver volume measurement using conventional methods (i.e., measurement of liver volume after sacrifice of the mice using a water displacement device) (Fig. 2A). The interobserver and intraobserver correlation coefficient for the native liver volumetry measured by MRI were 0.94 ($P < 0.001$; 95% confidence interval [CI], 0.80–0.98) and 0.85 ($P = 0.002$; 95% CI, 0.73–0.97), respectively (Fig. 2B and C).

3.2. Small animal MRI volumetry after 70% PH

The same MRI unit was then used to assess its accuracy in the determination of liver remnant volume after 70% PH. Twenty mice underwent 70% PH followed by MRI liver volumetry at four different time points of liver regeneration (day 2, 5, 7, and 10) before sacrifice. Overall, the MRI liver volumetry (Fig. 3A) correlated highly with the true liver volume measurements using the conventional technique (Pearson correlation coefficient, 0.98; 95% CI, 0.96–0.99; $P < 0.001$). The mean liver volume increased from day 2 to day 10 (1.1 SD ± 0.26 cm^3) reaching 80% of the native liver volume (Fig. 3B, D, and E). The interobserver correlation coefficient was 0.94 (95% CI, 0.90–0.97; $P < 0.001$) (Fig. 3C).

3.3. Liver volumetry dynamics after 70% PH

Because liver regeneration is a dynamic process, the next step was to analyze the dynamics of liver volume during liver regeneration after PH. For this purpose, we repeated MRI liver volumetry at different time points in six mice that underwent 70% PH. Liver hypertrophy started at day 1 after hepatectomy (volume of 0.67 ± 0.04 cm^3) and was maximal at day 10 (volume of 1.21 ± 0.13 cm^3) where the liver volumetry reached a plateau, corresponding to 83% of the original liver volume (Fig. 4A). This trend was comparable when the liver volumetry was adjusted to the mouse body weight (Fig. 4B).

To assess the impact of the potential stress induced by anesthesia and dehydration during the image acquisition by MRI, we analyzed a group of mice ($n = 6$) that underwent sham surgery with repetitive MRI liver volumetry at different time points. In this setting (Fig. 5A), we observed that the native liver volumetry by MRI decreased from 14% between days 0 and 1 (mean volume 1.39 ± 0.23 to 1.2 ± 0.14 cm^3). However, this volume loss was restored at day 2. These changes were comparable when liver volume was adjusted to the body weight (Fig. 5B).

3.4. Hepatocyte proliferation after 70% PH

Hepatocyte proliferation was assessed using Ki-67 and pH3 staining. Figure 6 shows that the peak of liver regeneration occurred at day 2 after 70% PH and correlated highly with the significant increase of liver volume demonstrated after day 2 (Fig. 3).

3.5. Analysis of intrahepatic vascular anatomy before and after PVE

In the same group of mice ($n = 16$), we compared consecutively MRA and portography before and after PVE of the median and

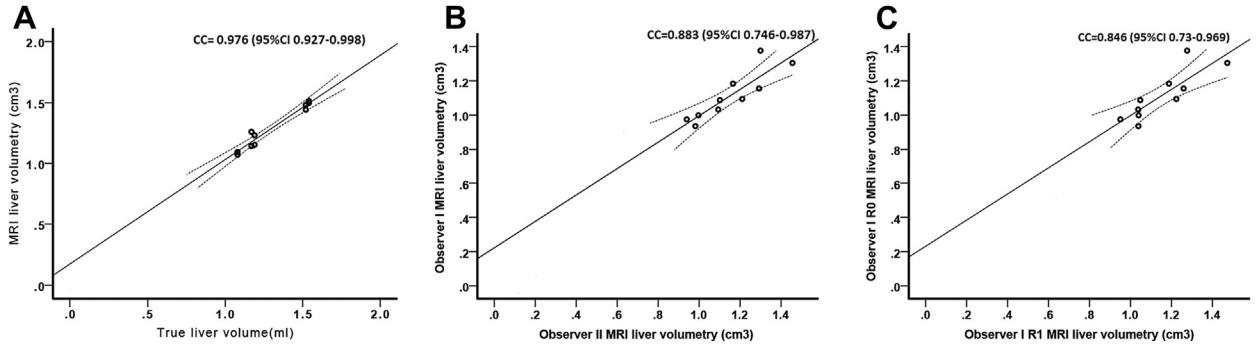

Fig. 2 – (A) MRI native liver volumetry *versus* true native liver volume measured by conventional methods ($n = 10$). MRI native liver volumetry highly correlates with the true liver volume (Pearson coefficient, 0.976; $P < 0.001$; 95% CI, 0.927–0.998). (B) Interobserver (E.M. and D.A.R.) correlation for the native liver volumetry by MRI. (C) Intraobserver correlation for the native liver volumetry by MRI. Dashed lines represent the 95% CI. CC, Pearson correlation coefficient; R0, initial results of liver volumetry by observer I; R1, results of liver volumetry reproduced by observer I.

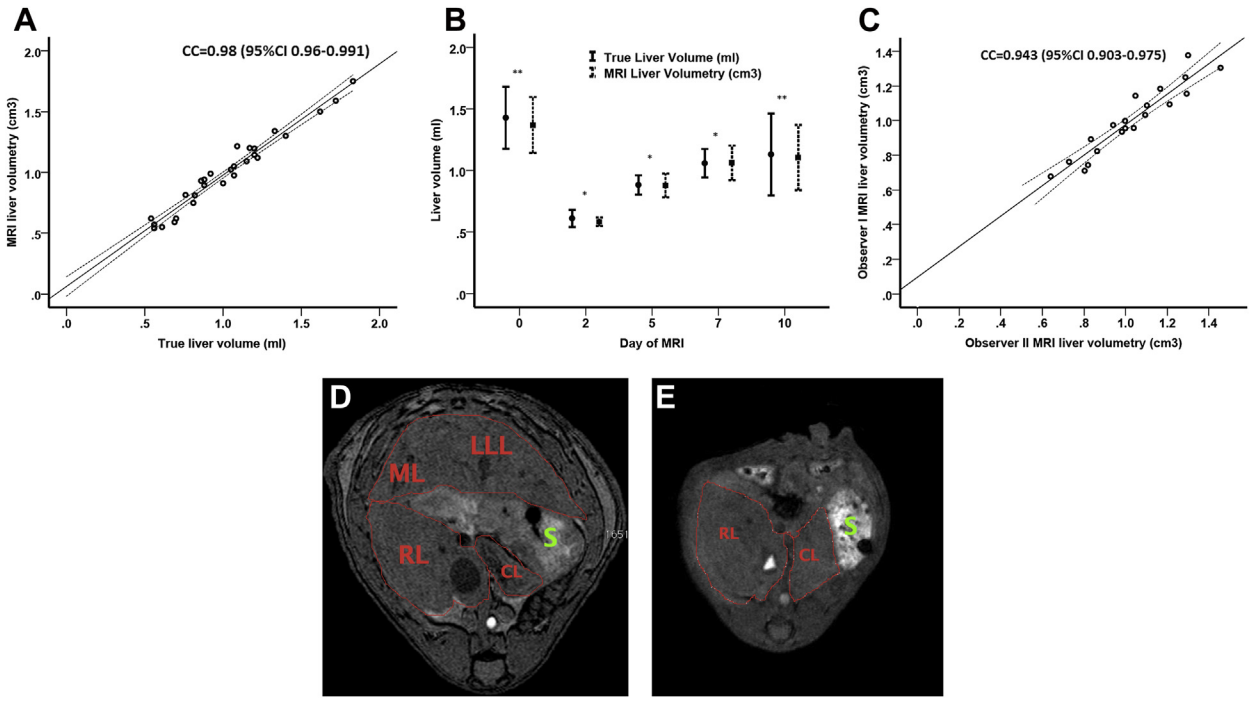

Fig. 3 – (A) Correlation between MRI liver volumetry *versus* true liver volume measured by conventional methods in mice treated and not treated with surgery at any time points ($n = 30$). (B) Liver volumetry by MRI *versus* true liver volume according to the postoperative day ($n = 20$). Mice at day 0 had no surgery ($n = 5$). (C) Overall interobservers correlation for the liver volumetry by MRI. (D, E) MRI liver volumetry before PH and 10 d after 70% PH in a single mouse. ML, medial lobe; LLL, left lateral lobe; RL, right lobe; CL, caudate lobe; S, stomach. Dashed lines represent the 95% CI. CC, Pearson correlation coefficient. Error bars indicate the standard deviation. **Correlation is significant at the 0.01 level. *Correlation is significant at the 0.05 level.

left lateral lobes (Fig. 7A and E). Using the water proton signal detected by the MRI, accurate imaging of the portal vein, inferior vena cava, and abdominal aorta were obtained without the need of an intravenous contrast injection (Fig. 7A and B). According to the two independent observers (C.T. and D.A.R.), the diagnostic accuracy of MRA and portography for occlusion of one branch of the portal vein was 0.95 (95% CI, 0.84–1) and 0.92 (95% CI, 0.73–1), respectively. Similarly, the level of agreement between the two observers for the description of intrahepatic vascular anatomy was excellent for MRA and portography (Cohen κ values = 0.925 and 0.862, respectively).

4. Discussion

In this report, we describe a novel imaging approach using MRI to assess liver volume and intrahepatic vascular anatomy in mice. Despite its small size, the mouse liver can be accurately and serially analyzed with minimal harm to the animal. Serial imaging, even over short periods, provides new insights into the dynamics of liver growth and vascular structure changes.

Liver regeneration after PH or occlusion of one portal vein vessel can be assessed exclusively in an *in vivo* model.

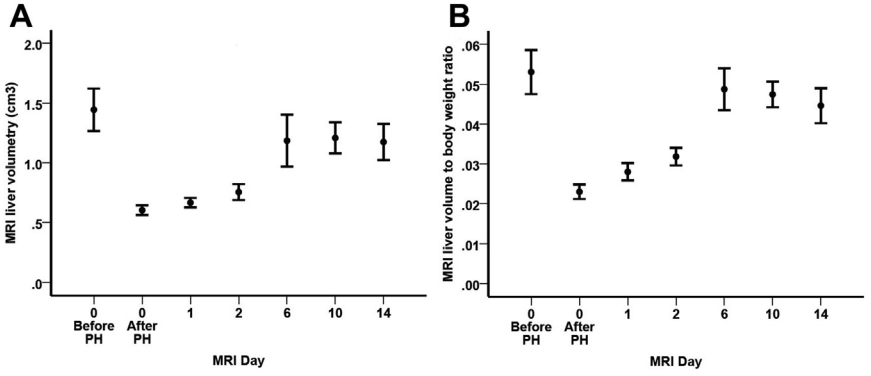

Fig. 4 – Dynamics of MRI liver volumetry after 70% PH in the same group of mice ($n = 6$). (A) Mean MRI liver volumetry according to the postoperative day. (B) Ratio of liver volumetry to the body weight according to the postoperative day. Error bars indicate the standard deviation. PH, partial hepatectomy.

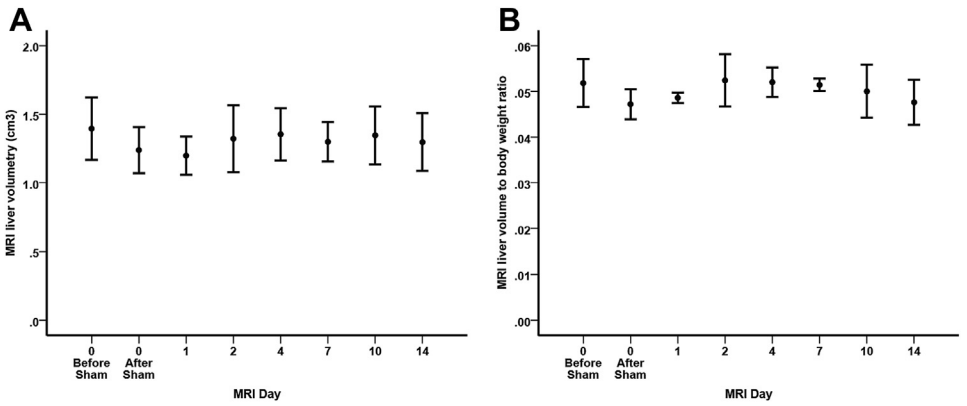

Fig. 5 – (A) MRI liver volumetry dynamics according to the day after sham surgery ($n = 6$). (B) Ratio of MRI liver volumetry to the body weight after sham surgery. Error bars indicate the standard deviation.

Currently, conventional approaches require invasive methods including sacrifice of mice at each time point to assess the liver hypertrophy. This implies the use of a large number of animals for analysis. Thus, MRI might be a highly attractive tool to provide repetitive analyses of liver morphology in a single mouse. Moreover, MRI has a great advantage over x-ray–based techniques, because it avoids tissue damage through harmful repetitive x-ray exposure.

We observed that the small animal MRI provides similar data as a conventional method associated with autopsy of the animal to assess the volume of the native liver and regenerating liver after PH. These results are consistent with two previous experimental studies in mice using MRI [12,14]. However, one study assessed different types of hepatectomy at only one postoperative time point [12], precluding a true dynamic evaluation of the liver volume during liver regeneration and the other study included only six mice [14]. Although the use of contrast agents for MRI liver volumetry is still debated, contrast was not a key element of our protocol. Indeed, most authors agree that to perform an intravenous contrast injection in mice requires skills, and unsuccessful or incomplete injections may occur [12,13]. In addition, anesthesia might influence the kinetics of a contrast agent and hence the optimal scan timing for liver volumetry [13]. Our results showed that the use of a contrast agent is not crucial for MRI liver volume measurement in native or hypertrophied livers after PH.

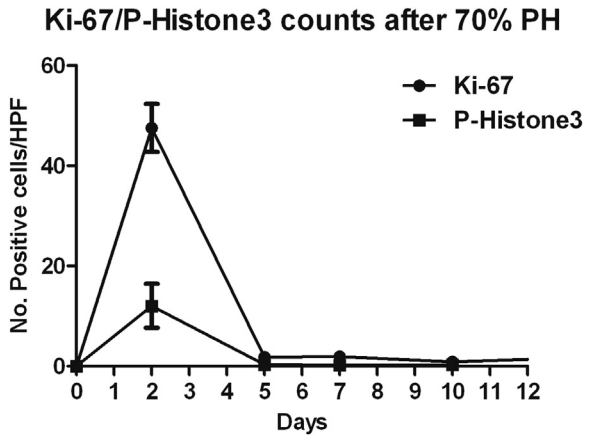

Fig. 6 – Time course of labeling indexes for Ki-67 (solid circles) and pH3 (solid squares) in hepatectomized livers. Error bars indicate the standard deviation.

Interestingly, although an injection of the contrast agent may be intuitively useful for angiographic imaging of the liver, we also observed that MRA without contrast is as accurate as the use of x-ray–based techniques with contrast agents (i.e., portography and microCT) to produce high quality imaging of the portal vein before or after the selective occlusion of its tributaries. Indeed, MRA uses the water proton signal to produce millimeter-scale images of arteries and veins without the addition of contrast agents [20]. Portography performed under general anesthesia requires a laparotomy, puncture of the portal vein, and injection of contrast agents under repetitive x-rays control. It is technically demanding and requires sacrifice of animals. Similarly, microCT requires peripheral injection of contract agents, which is technically demanding in rodents [9]. Finally, inherent toxicities of contrast agents might harm mice having undergone manipulations of the liver, particularly when critical volumes are resected, that is, more than 70%. For all these reasons, MRA appears very attractive because it allows repetitive assessment of the portal vein without injection of any contrast agents and without sacrificing animals.

OsiriX is an open source image processing software that has been validated in many fields of application in clinical settings [21,22]. Because its access is free, it can be used worldwide and has been shown to be very convenient and easy to use for the analysis of DICOM images. This software facilitates the assessment of vascular changes after hepatectomy or portal vein manipulation. Indeed, these changes including shunts, thrombosis, or recanalization are important to understand the underlying mechanism of liver regeneration.

These protocols described herein could also be used for the assessment of growing and hypervascularized masses (e.g., tumor masses) and other organs such as kidneys, prostate, and ovaries [10,11,18]. Strong correlations were demonstrated between MRI and necropsy-determined tumor masses in mice [10]. For instance, MRI assessment of the volume of the mouse

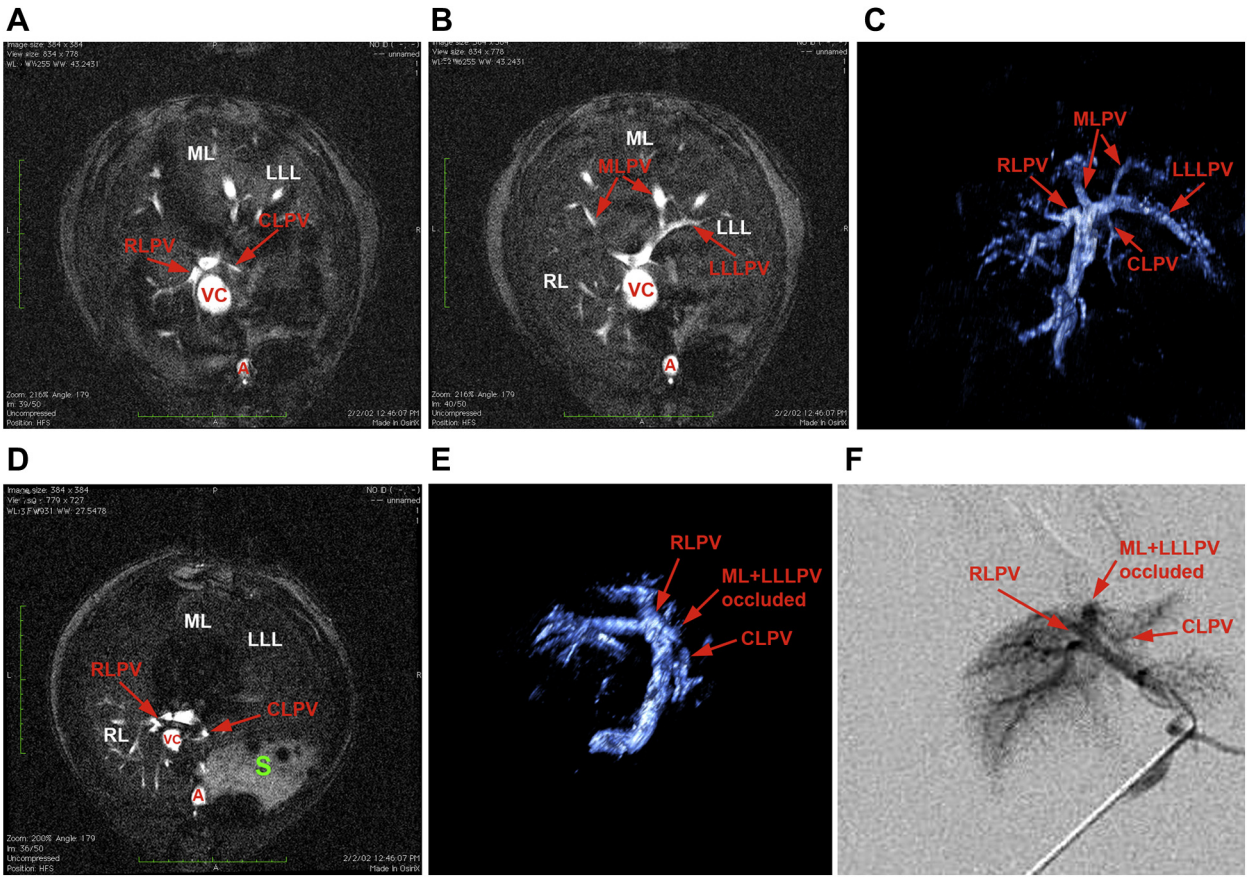

Fig. 7 – MRI of the portal vein branches before (A, B) and after (D) PVE. Three-dimensional reconstruction of the portal vein using OsiriX software before (C) and after (E) PVE. Portography after PVE in the same mouse (F). In (D) and (E), the branches to the median and left lateral lobes are occluded by the Embospheres. Portography (F) correlates positively with the images acquired by MRI and analyzed with the OsiriX software (E). MLPV, median lobe portal vein; RLPV, right lobe portal vein; CLPV, caudate lobe portal vein; LLLPV, left lateral lobe portal vein; S, stomach.

prostate is also precise and reproducible [11]. Our protocols may then bring new insights in the assessment of growing masses and organ volume in small animals, with precise 3D vascular mapping.

The primary aim of this study was to assess the efficiency of small animal MRI for liver hypertrophy measurement and portal vein anatomy evaluation in mice. However, this technique can be applied in clinical situations where the FRL volume needs to be assessed before or after any hepatectomy or where anatomic variations of liver vascularization need to be ruled out before portal vein manipulations. This technique can be used in the setting of living donor liver transplantation or a liver tumor requiring a major hepatectomy. In addition, based on the proposed protocol, this noninvasive technology will serve the dynamic study of new strategies to enhance liver regeneration *in vivo* (e.g., associating liver partition and portal vein ligation for staged hepatectomy).

Of note, in mouse experiments for accurate volumetry a much higher spatial resolution is required compared with the evaluation of human subjects. This is the reason why small animal scanners typically exhibit higher static magnetic field strength [23]. The achievable signal-to-noise ratio in theory linearly scales with both the field strength and the voxel size. Therefore, for small voxel size the field strength needs to be higher for equal image quality. In humans, the same (relative) accuracy should easily be achieved using a clinical scanner at 1.5 or 3 T. If the same volumetry in mice is performed at a clinical magnetic resonance scanner, at least a dedicated birdcage mouse coil is necessary to achieve a sufficient signal-to-noise ratio.

One of the major limitations of the small animal MRI or MRA technology is its cost. Depending on the magnetic strength, systems used for animal imaging between 1.5 and 14 T in magnetic flux density range from $1 million to more than $6 million, with most systems costing around $2 million. Furthermore, the image acquisition time may be long, and hence may negatively affect animals that are anesthetized for long periods. In addition, small animal MRI typically captures a snapshot of the subject in time, making important information such as blood flow velocity quantification difficult to assess.

5. Conclusions

To sum up, the small animal MRI is an accurate tool to assess both liver hypertrophy during liver regeneration and

corresponding modifications of intrahepatic vascular anatomy in mice. This method is noninvasive, reproducible, and allows serial evaluation of the liver without the need to sacrifice animals. It is of great interest for the development of new agents to improve liver regeneration. In addition, it may help to better characterize morphologic and vascular changes in other organs in experimental small animal models.

Acknowledgment

This research is funded by the Swiss National Fund (SNF) (record no. PP00P3_128475) and was supported by the Clinical Research Priority Program of the University of Zurich Molecular Imaging Network Zurich (MINZ).

REFERENCES

[1] Clavien PA, Petrowsky H, DeOliveira ML, Graf R. Strategies for safer liver surgery and partial liver transplantation. N Engl J Med 2007;356:1545.
[2] Makuuchi M, Thai BL, Takayasu K, et al. Preoperative portal embolization to increase safety of major hepatectomy for hilar bile duct carcinoma: a preliminary report. Surgery 1990;107:521.
[3] Abulkhir A, Limongelli P, Healey AJ, et al. Preoperative portal vein embolization for major liver resection: a meta-analysis. Ann Surg 2008;247:49.
[4] Furrer K, Tian Y, Pfammatter T, et al. Selective portal vein embolization and ligation trigger different regenerative responses in the rat liver. Hepatology 2008;47:1615.
[5] Lainas P, Boudechiche L, Osorio A, et al. Liver regeneration and recanalization time course following reversible portal vein embolization. J Hepatol 2008;49:354.
[6] Lesurtel M, Belghiti J. Temporary portal vein embolization as a starter of liver regeneration. J Hepatol 2008;49:313.
[7] Aussilhou B, Lesurtel M, Sauvanet A, et al. Right portal vein ligation is as efficient as portal vein embolization to induce hypertrophy of the left liver remnant. J Gastrointest Surg 2008;12:297.
[8] Prajapati SI, Keller C. Contrast enhanced vessel imaging using microCT. J Vis Exp 2011;47:2377.
[9] Fiebig T, Boll H, Figueiredo G, et al. Three-dimensional in vivo imaging of the murine liver: a micro-computed tomography-based anatomical study. PLoS One 2012;7:e31179.
[10] Montelius M, Ljungberg M, Horn M, Forssell-Aronsson E. Tumour size measurement in a mouse model using high resolution MRI. BMC Med Imaging 2012;12:12.
[11] Nastiuk KL, Liu H, Hamamura M, Muftuler LT, Nalcioglu O, Krolewski JJ. *In vivo* MRI volumetric measurement of prostate regression and growth in mice. BMC Urol 2007; 7:12.
[12] Inderbitzin D, Gass M, Beldi G, et al. Magnetic resonance imaging provides accurate and precise volume determination of the regenerating mouse liver. J Gastrointest Surg 2004;8:806.
[13] Inoue Y, Yoshikawa K, Nomura Y, et al. Gadobenate dimeglumine as a contrast agent for MRI of the mouse liver. NMR Biomed 2007;20:726.
[14] Garbow JR, Kataoka M, Flye MW. MRI measurement of liver regeneration in mice following partial hepatectomy. Magn Reson Med 2004;52:177.
[15] Rosset A, Spadola L, Pysher L, Ratib O. Informatics in radiology (infoRAD): navigating the fifth dimension: innovative interface for multidimensional multimodality image navigation. Radiographics 2006;26:299.
[16] Lesurtel M, Graf R, Aleil B, et al. Platelet-derived serotonin mediates liver regeneration. Science 2006;312:104.
[17] Pache JC, Roberts N, Vock P, Zimmermann A, Cruz-Orive LM. Vertical LM sectioning and parallel CT scanning designs for stereology: application to human lung. J Microsc 1993; 170(Pt 1):9.
[18] Hensley HH, Roder NA, O'Brien SW, et al. Combined in vivo molecular and anatomic imaging for detection of ovarian carcinoma-associated protease activity and integrin expression in mice. Neoplasia 2012;14:451.
[19] Cornelissen B, Kersemans V, Jans L, et al. Comparison between 1 T MRI and non-MRI based volumetry in inoculated tumours in mice. Br J Radiol 2005;78:338.
[20] Walter T, Shattuck DW, Baldock R, et al. Visualization of image data from cells to organisms. Nat Methods 2010;7(3 Suppl):S26.
[21] Volonte F, Pugin F, Bucher P, Sugimoto M, Ratib O, Morel P. Augmented reality and image overlay navigation with OsiriX in laparoscopic and robotic surgery: not only a matter of fashion. J Hepatobiliary Pancreat Sci 2011;18:506.
[22] Volonte F, Robert JH, Ratib O, Triponez F. A lung segmentectomy performed with 3D reconstruction images available on the operating table with an iPad. Interact Cardiovasc Thorac Surg 2011;12:1066.
[23] Schick F. Whole-body MRI at high field: technical limits and clinical potential. Eur Radiol 2005;15:946.